Sensors & Actuators: A. Physical 369 (2024) 115223

Contents lists available at ScienceDirect

Sensors and Actuators: A. Physical

journal homepage: www.journals.elsevier.com/sensors-and-actuators-a-physical

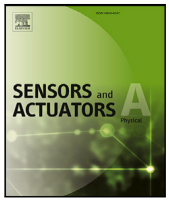

Enhanced aroma prediction in coffee fermentation through optical fiber sensor data fusion

Renato Luiz Faraco Filho *, João Victor de Castro, Felipe Oliveira Barino, Deivid Campos, Alexandre Bessa dos Santos

Instrumentation and Telemetry Laboratory, Federal University of Juiz de Fora, 36036-900, Brazil

ARTICLE INFO

Keywords:
Aromas
Carbon dioxide
Coffee
Fermentation
Interferometer
Temperature
Fiber grating
Optical sensor

ABSTRACT

This study presents the development of a monitoring probe for characterizing aromas during the coffee fermentation process. Using an optical device created through a Twin Long Period Fiber Grating interferometer in conjunction with auxiliary measurements of carbon dioxide and temperature, the probe was designed to capture relevant data throughout the fermentation process. A set of analyses were conducted, examining carbon dioxide levels, temperature, and spectral analysis, to effectively identify and classify aromas. The results demonstrate that the developed device proved to be a promising tool for monitoring and characterizing the coffee fermentation process. Furthermore, this work opens perspectives for the application of sensors and monitoring techniques in industrial processes, with the potential to enhance quality and efficiency in agro-industry.

1. Introduction

Coffee is one of the most popular beverages globally, consumed by billions of people every day. According to Lee et al. [1] global coffee consumption has consistently increased, with an average annual growth of 1.9% over the last 50 years. Additionally, coffee is among the most traded commodities worldwide, with coffee consumption reaching 175.6 million bags in 2022 and projected for 2023 [2]. Furthermore, coffee plays a crucial role in the Brazilian economy, as Brazil stands as the world's largest producer and exporter of coffee [3].

The coffee fermentation process is a pivotal stage in coffee production, influencing the taste and aroma of the beverage and consequently its market value. Moreover, the intricate relationship between the coffee bean fermentation process and the aroma profile is a crucial element to consider. Fermentation is responsible for producing volatile compounds that contribute to the diversification and enhancement of coffee aroma and flavor [4–8].

However, due to the lack of precise control and monitoring, the fermentation process is exceedingly complex. It is noteworthy that factors such as fermentation time, temperature, and pH significantly influence the final result, posing substantial challenges that need to be addressed to ensure the quality and consistency of the produced coffee [9,10]. In this challenging and crucial scenario of coffee production, the pursuit of innovative and accurate monitoring solutions becomes paramount.

To precisely monitor and control the complex coffee fermentation process, we leverage advanced technologies and pattern recognition methods within the domain of data mining. By using data mining techniques, such as Principal Component Analysis (PCA), it is possible to analyze large datasets collected during the fermentation process to identify patterns and relationships that would be difficult to detect manually. This allows us to develop sensors and other tools that can monitor key parameters in real-time and provide precise information into the quality and consistency of the final coffee product.

An intriguing solution for this case is electronic odor sensors [11–13], also known as e-noses, proving to be a promising tool for the coffee industry and other agricultural sectors [14].

Undoubtedly, electronic odor sensors have been successfully used in various applications in the food industry [15,16], agricultural sectors [17,18], including the coffee fermentation process [19]. Additionally, numerous studies have demonstrated correlations between the chemical properties of the analyzed medium and odor descriptors [20–22].

As a rule, electronic odor descriptors are manufactured from a set of gas sensors using conductive polymers, metal-oxide semiconductors, quartz crystal microbalance, and surface acoustic wave sensors designed to identify a range of volatile organic compounds [23]. However, electronic devices have disadvantages due to their high sensitivity to temperature, humidity, pressure, and gas flow, leading to imprecise measurements and compromising device reliability.

Thus, the advantages presented by fiber optic sensors (FOS) become evident. These devices are less susceptible to noise, do not

* Corresponding author.
E-mail address: renato.luiz@engenharia.ufjf.br (R.L.F. Filho).

https://doi.org/10.1016/j.sna.2024.115223
Received 8 December 2023; Received in revised form 2 February 2024; Accepted 24 February 2024
Available online 27 February 2024
0924-4247/© 2024 Elsevier B.V. All rights reserved.

oxidize, are immune to electromagnetic interference, and are lightweight and compact [24]. Long Period Fiber Gratings (LPFGs) have been widely used for applications involving refractive index sensing [25,26], humidity [27,28], gases [29,30], and quality control applications [31].

Moreover, the combination of two similar LPGs can be used to construct interferometers with improved sensitivity parameters [32]. This results in a complex optical transmission spectrum that favors multi-parametric and self-compensating measurements [33,34].

In this study, we developed an optical nose through a set of Twin Long Period Fiber Grating interferometers constructed using two series-coupled micro-tapered Long Period gratings (MT-LPFGs). The device was utilized to collect data from the coffee fermentation process, coupled with auxiliary measurements of carbon dioxide (CO_2) and temperature. For temperature readings, the BMP280 sensor was employed. The measurement of carbon dioxide levels was facilitated by the CCS811 CO_2 sensor, with the aim of monitoring and improving the coffee fermentation process. Throughout this article, we will present the development of the optical nose, the results of the obtained measurements, and the integration of the collected data with auxiliary measurements of CO_2 and temperature taken during the fermentation process. The results obtained indicate that the developed apparatus is a promising tool for aroma classification in the coffee fermentation process, contributing to both efficiency and quality enhancement.

2. Methods

2.1. Probe assembly

LPFG's are created through the intermittent modification of optical fiber characteristics, such as refractive index and geometry. This periodic alteration ranges typically from several tens to hundreds of micrometers [35]. This periodic arrangement facilitates the transition of the guided mode from the fiber core to evanescent cladding modes. As scattering occurs at the junction between the cladding and the external medium, there is a loss of optical power at the wavelength at which light is coupled. This particular wavelength is termed the resonant wavelength (λ_{res}) and can be determined by [35,36]:

$$\lambda_{res}^{m} = (n_{eff,co} - n_{eff,cl}^{m}).\Lambda \tag{1}$$

where λ_{res}^{m} represents the mth resonant wavelength, Λ stands for the grating period, $n_{eff,co}$ denotes the effective index of the core mode, while $n_{eff,cl}^{m}$ signifies the effective index of the mth cladding mode. By combining two cascaded identical LPGFs, it is possible to fabricate in-fiber Mach–Zehnder interferometers (MZIs). Their operating principle is based on the first LPFG coupling a fraction of the core light into the cladding modes, and subsequently, the second LPFG, positioned at a minimum distance, recoupling the cladding modes' light back into the core [37]. The analysis of the output signals from the MZIs is described by Eqs. (2) and (3)

$$\phi(t)_{MZI} = \frac{2\pi\delta n_{eff}^{m} L_{cav}}{\lambda} \tag{2}$$

$$I_{MZI} = 1 - 4T_{core}T_{clad}.sen^{2}\left(\frac{\pi\delta n_{eff}^{m} L_{cav}}{\lambda}\right) \tag{3}$$

where $\phi(t)MZI$ is the phase variation in the interferometer, δ is the optical path difference, $Lcav$ is the length of the resonant cavity, and λ is the wavelength of incident light. Additionally, I_{MZI} represents the light intensity in the MZI, while T_{core} and T_{clad} denote the transmission factors through the core and cladding, respectively. It is important to highlight that in a Mach–Zehnder interferometer system, the relationship between the refractive index of the medium (n) and the length of the medium can be inferred from Eq. (4)

$$n = \frac{\lambda\Delta\phi}{2\pi d} \tag{4}$$

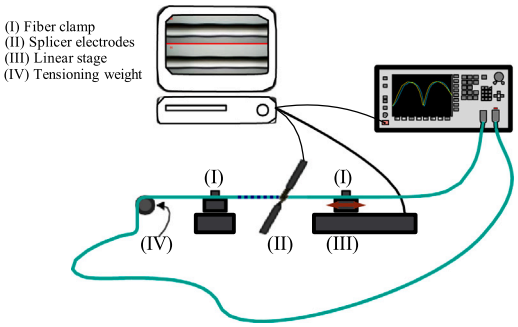

Fig. 1. Electric arc method manufacturing schematics.

where $\Delta\phi$ is the phase difference between the two interference patterns, and d is the length of the medium. Since, it is difficult to obtain the value of $\Delta\phi$, but the variation amplitude of fringes can be measured directly and accurately, Liu et al. [38], proved that, the refractive index n can be expressed by the fringe variation ($s(r)$) and the stripe width (D) as shown in Eq. (5):

$$n = \frac{\lambda s(r)}{d D} \tag{5}$$

For the manufacturing of the probe used, a twin LPFG interferometer, composed of two cascaded MT-LPFGs, was developed. In this way, the FOS was crafted using the electric arc method. The choice of the tapering method is driven by our aim to maintain consistency with devices used in a prior study [19], which successfully employed a similar approach. Also, it is worth noting that several studies have highlighted the strong performance of arc-induced long-period fiber gratings for refractive index [39–42]. While there may be limited research specifically on LPGs in coffee fermentation, refractive index and Brix parameters play a crucial role in assessing the quality of the fermentation process [43–46].

Generally speaking, arc induced gratings are fabricated by placing an uncoated fiber, under tension, between the electrodes of a splicing machine [47]. To achieve this, an optical splicing machine adapted for LPFG sensor production was utilized. A schematic representation of the manufacturing process is illustrated in Fig. 1. This process closely follows the fabrication technique described in [48]. In brief, the optical fiber is meticulously positioned between the electrodes of a splicing machine. One end of the fiber is securely clamped in a fiber holder atop a translation stage, ensuring control along the z-axis. Simultaneously, a mass is attached to the other end to maintain the fiber under a consistent axial tension. The electric discharge is then initiated. Subsequently, the fiber is incrementally moved over the grating period. These last two steps are iteratively repeated, with the entire process.

The electric arcs, were generated using a pre-configured machine. This machine was set up according to the standards discussed in [49], where the configurations of the electric arcs were carefully fine-tuned through iterative experimentation. It is noteworthy that the particular settings adopted from [49] were instrumental in achieving superior spectral quality in the sensors, ensuring attributes such as low attenuation during manufacturing. Simultaneously, the choice of the period for the micro-tapered Long Period Fiber Gratings (MT-LPFGs) at 500μm was informed by experiments detailed in [50]. This specific period was strategically selected as it results in a resonant wavelength of approximately 1480 nm. This wavelength is proximate to the peak wavelength of the SLED source used in our study (1550 nm), aligning our sensor with the characteristics of the light source.

Two protective capsules for the sensors were designed to keep the sensors stable in the barrel, preventing any potential mechanical interferences. One capsule is dedicated to housing the optical device, while the other encapsulates the sensors responsible for auxiliary measurements. The primary objectives of these capsules are for shielding

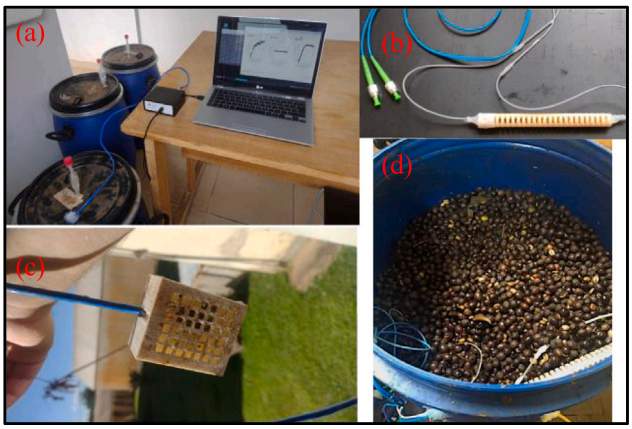

Fig. 2. (a) Experimental setup, (b) Protective capsule for optical sensor, (c) Protective capsule for auxiliary sensors, (d) Fermentation barrel with coffee beans and sensors.

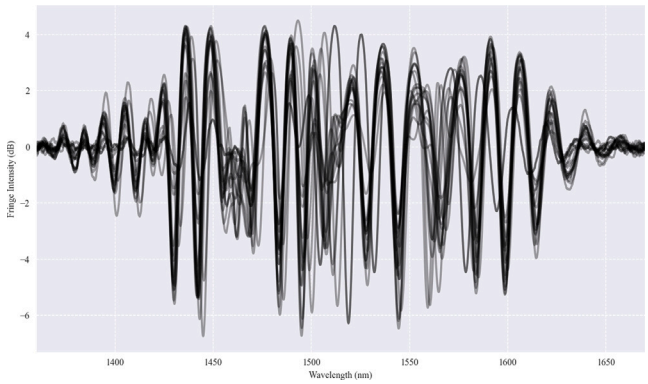

Fig. 3. Dynamic evolution of interference spectra during coffee fermentation.

and isolating the sensitive region of the optical fiber from direct contact with coffee beans. Both capsules were crafted using poly-lactic acid (PLA) through fused deposition modeling (FDM). The protective capsule for the optical device is showcased in the intricate 3D model presented in Fig. 2(b), while the capsule for the electronic sensors responsible for auxiliary measurements is detailed in Fig. 2(c). The design of openings in these enclosures allows the entry of gases while safeguarding the sensors from direct contact with coffee beans.

Furthermore, for data acquisition, a hardware system was designed to interact with the probe, capturing signals from temperature and humidity sensors and storing them in a database for future analysis. In conjunction with this equipment, software was also developed to enable real-time data visualization for the operator.

2.2. Experimental setup

The setup for monitoring the fermentation process included the probes, hardware, and software developed. Additionally, for the use of optical devices, an Opto-Link 1550 nm SLED source and a Thorlabs Fourier Transform Optical Spectrum Analyzer OSA203 were employed to acquire the optical spectrum.

Coffee beans were selected through selective harvesting, ensuring 100% maturity and minimizing impurities such as leaves and branches. For the fermentation process, the yeast-to-grain ratio was 1:100, leading to dilution occurring concurrently with the coffee inside the bioreactor (a $50L$ barrel).

Given the potential risk of damage to the sensors from contact with the wort produced during the fermentation process, the probes were positioned at the top of the bioreactor, maintaining a distance of 10 cm above the coffee beans and yeast solution. This way, the devices measured gases produced during the fermentation process, responding to variations in odor throughout the process. Subsequently, the barrel was sealed following good fermentation practices and only opened for aroma verification. It is noteworthy that the process was halted when the optimal aroma was perceived. Consequently, the fermented beans exhibited two significant aromas, fruity and alcoholic. Fig. 2(a) illustrates the data collection process during fermentation, providing an overview of our experimental setup. Fig. 2(d) shows the placement of the probes on the coffee beans.

2.3. Optical data analysis

For the proper analysis of optical spectra, the collected data were initially processed by extracting interference fringes. Subsequently, noise reduction was performed using Savitzky–Golay (SVG) filters. Later, a moving average (M.A.) filter with an order (N) of 100 was applied to obtain the average power spectrum. Subsequently, the resulting spectrum was obtained by subtracting the average power spectrum from the spectrum smoothed by the SVG filter. Fig. 3 presents the interference spectrum obtained after applying the processing techniques. On the X-axis, we have the wavelength of the incident light (in nm), while the Y-axis represents the intensity of the interference fringes (in dB). The figure highlights a significant alteration in the optical spectrum throughout the experiments, allowing for the visualization of fringe variation over time at different wavelengths. We can observe the transition from darker to lighter traces, indicating the optical device's sensitivity to changes in coffee characteristics during the fermentation process. An interesting approach to optical spectrum processing involves extracting resonant wavelengths from each interference fringe. However, due to the complexity of the analyzed process, coupled with the non-linearity in spectral variation throughout the experiment, this method proved unattractive. Thus, to facilitate a preliminary analysis of results, only a spectrogram was created, illustrating the wavelength variation along with the fringe intensity over the fermentation time.

Moreover, aiming to reduce dimensionality and provide a more in-depth analysis of the data, interference fringes were processed through Principal Component Analysis (PCA). Due to the large number of input variables, this technique becomes appealing as it can encapsulate the entire dataset. Thus, the collected spectra were concatenated and processed, maximizing the utilization of available data. PCA is a useful statistical technique, and is a common method for finding patterns in data of high dimension [51,52]. In the context of our study, PCA identified the principal components, which are linear combinations of the original input variables. These principal components capture the most significant variability in the dataset. The first two principal components, labeled PC1 and PC2, were selected as they represent the directions of maximum variance and exhibit the highest correlation with the primary data. Also, using the complete spectrum prevents the loss of input features caused by attenuation, coupling, or resonant wavelength loss due to the high sensitivity of optical devices.

Finally, the processed data were associated with the temperature and CO_2 measurements over the fermentation time throughout the process. It is important to note that the non-uniform spectrum of the interference pattern can be explained by the manufacturing method used. Thus, periodic fluctuations occur and accumulate over several periods required to achieve the desired transfer characteristic. Additionally, the splicing machine used may introduce minor inconsistencies between each period. However, this does not compromise the spectral analysis but rather makes each MT-LPFG unique.

3. Results

Initially, the verification of CO_2 and temperature measurements throughout the fermentation process was carried out and associated

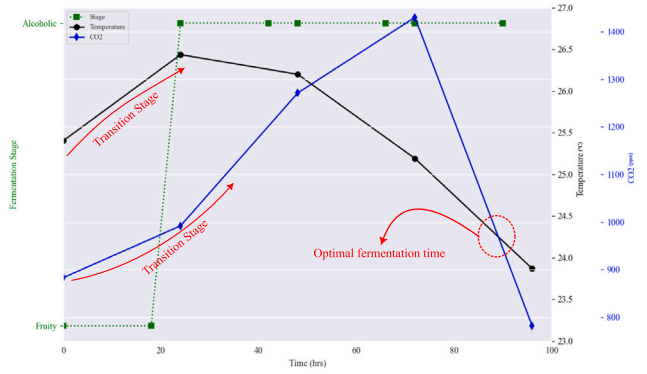

Fig. 4. Time series for CO_2 and temperature.

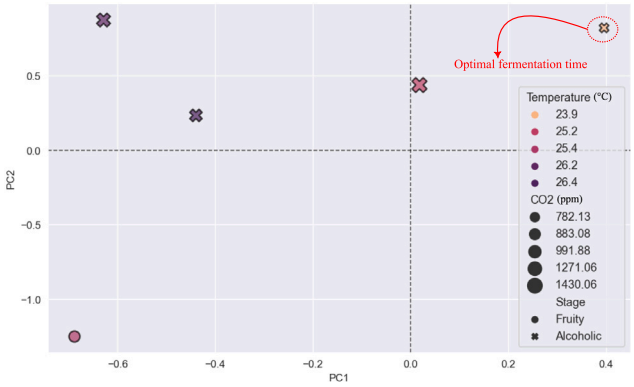

Fig. 6. PCA results.

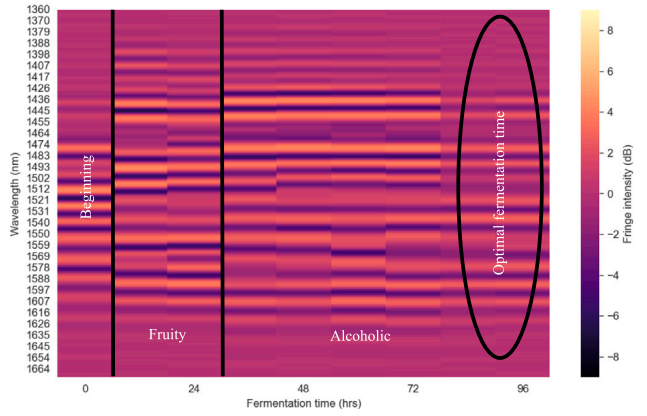

Fig. 5. Spectrogram of the optical device during the fermentation process.

with the coffee aroma. It was observed that during the transition between fruity and alcoholic aromas, there was a significant increase in CO_2 and temperature levels, which then decreased until the optimal alcoholic aroma was reached. It is important to note that CO_2 levels reduced more abruptly throughout the process. Fig. 4 presents the time series for the preliminary analysis of CO_2 and temperature throughout the experiment, showing the transition between odors and the moment when the beans reached the ideal aroma.

The aromas were defined and classified through human sensory evaluation. Hence, over the days, an expert assessed the aroma of the beans until identifying the ideal aroma, marking the optimal fermentation moment. Among these classifications, the optimal fermentation moment was determined when the beans exhibited an alcoholic aroma, reminiscent of brandy, with notes of cinnamon, chocolate, while retaining the coffee aroma. Subsequently, CO_2 and temperature measurements were associated with the aroma classification defined by the expert and concatenated into the time series presented in Fig. 4. This image reveals a significant increase in temperature and CO_2 levels during the transition from fruity to alcoholic aromas. It also demonstrates a decline in these measures when the ideal aroma was achieved. It is essential to note that the process lasts approximately 96 h, and each point on the graph represents the daily average of each measure, considering that these indices can vary considerably throughout the day. The experiments were conducted in a controlled environment to ensure consistent conditions, and the bioreactors were maintained in a controlled atmosphere.

Fig. 5 shows the spectrogram that reveals variations in wavelengths and intensity of interferometric fringes over time. On the *y*-axis, the wavelength of the incident light is presented in nanometers, while the *x*-axis represents the fermentation time in hours. The colors within the graph correspond to the fringe intensity, offering a visual indication of the changes over time. It shows a significant shift in the wavelengths of attenuation valleys during the aroma variation, allowing the identification of the emergence of the fruity aroma after the start of the process. However, despite presenting variations, distinguishing between fruity and alcoholic odors solely through the spectrogram proved to be a more complex task, as the variations in intensity and wavelength were not as significant. Also, despite no abrupt changes in wavelength, there was an increase in fringe intensity during the optimal fermentation period.

The results of Principal Component Analysis (PCA) indicated that, by employing this technique, the complexity of the dataset was reduced. The total variance explained by the principal components PC1 and PC2 is 57.37%, indicating that a significant percentage of the original variability in the data was retained.

Crucially, in this case, only one principal component would be needed to achieve 95% of the total variability. This suggests that using only PC1 would significantly simplify the dataset while retaining a substantial amount of the original information, which can be useful in contexts where simplicity and efficiency are priorities.

Fig. 6 illustrates the outcomes of Principal Component Analysis (PCA) obtained by spectral processing concerning the associated levels of temperature and CO_2. The distinct shapes, crosses, and circles, represent different aroma profiles, with crosses indicating predominantly alcoholic aromas and circles indicating fruity aromas. The colors within these shapes convey temperature variations (in °C), while the sizes are indicative of CO_2 concentrations (in ppm), where larger sizes denote higher levels. This visual representation effectively demonstrates the capability of the optical sensor to distinguish between various aromas based on the integration of PCA results with auxiliary data. Furthermore, this integration allows for the identification of the optimal fermentation moment by associating temperature and CO_2 with PCA outcomes, this association facilitates the recognition of variations in indices shortly after changes in odor patterns.

4. Conclusions

The research presented in this study demonstrates that the use of Fiber Based Twin Long Period Fiber Grating Interferometry is highly efficient in identifying nuances in the coffee fermentation process. The examination of CO_2 and temperature measurements throughout the fermentation process, coupled with coffee odor patterns, revealed significant correlations. During the transition between fruity and alcoholic aromas, a substantial increase in CO_2 and temperature levels was observed, followed by a decrease until reaching the optimal point for the ideal alcoholic odor. The significant shift in wavelength of attenuation valleys coincides with aroma changes, notably the transition to the

fruity aroma. However, distinguishing specific nuances solely through the spectrogram can be challenging due to the complexity of variations.

The application of PCA effectively reduced the dataset complexity, preserving 57.37% of the original variability with only two principal components. Thus, the discriminating potential of PCA concerning temperature and CO_2 levels, allowing clear differentiation between different aromas, is noteworthy. The integration of auxiliary data with the optical device shows promise in defining the ideal fermentation moment, as the association of temperature and CO_2 with PCA results enables the identification of changes in indices after alterations in odor patterns.

Collectively, these conclusions strengthen the understanding of the coffee fermentation process, emphasizing the importance of environmental variables and the potential of the analytical techniques used to monitor and optimize production, contributing to the desired sensory quality. These findings not only expand knowledge about product quality but also offer practical insights to enhance production methods.

These results pave the way for the development of real-time monitoring products that would replace traditional laboratory processes, making the quality control of the coffee fermentation process more efficient and precise. Therefore, this study highlights not only the effectiveness of fiber sensors in evaluating fermented coffee quality but also the promise of future innovations that could revolutionize the agro-industrial sector.

Building upon the obtained results, we find it compelling to delve deeper into this approach in future studies. An envisioned extension of this work involves integrating supplementary sensors to measure additional pertinent volatile compounds in coffee. We also aim to focus on the potential instability in the repeatability of the presented sensor. The consideration of a superior demodulation algorithm could be pivotal in compensating for any instability in the sensor's repeatability.

CRediT authorship contribution statement

Renato Luiz Faraco Filho: Writing – review & editing, Writing – original draft, Visualization, Validation, Methodology, Investigation, Formal analysis, Data curation, Conceptualization. **João Victor de Castro:** Methodology, Investigation, Formal analysis, Data curation. **Felipe Oliveira Barino:** Validation, Methodology, Investigation, Formal analysis, Data curation. **Deivid Campos:** Visualization, Validation, Methodology, Investigation, Formal analysis, Data curation. **Alexandre Bessa dos Santos:** Writing – review & editing, Visualization, Resources, Project administration, Funding acquisition, Conceptualization.

Declaration of competing interest

The authors of this submission declare that they have no financial or personal relationships with individuals or organizations that could potentially bias their work. No conflicts of interest, including employment, consultancies, stock ownership, honoraria, paid expert testimony, and grants or other funding, exist. All authors, including those without competing interests, confirm the absence of relevant financial and personal relationships. This declaration is submitted on behalf of all authors involved in the submission.

Data availability

Data will be made available on request.

Acknowledgments

We would like to express our gratitude to Capes, Brazil, CNPq, Brazil, Fapemig, Brazil, and Inerge, Brazil for their support, which greatly facilitated the successful completion of this work

References

[1] L.W. Lee, M.W. Cheong, P. Curran, B. Yu, S.Q. Liu, Coffee fermentation and flavor – an intricate and delicate relationship, Food Chem. 185 (2015) 182–191, http://dx.doi.org/10.1016/j.foodchem.2015.03.124.

[2] International Coffee Organization, Coffee production by exporting countries, 2023.

[3] I.C. Organization, Trade statistics tables, 2023.

[4] M. Haile, W.H. Kang, The role of microbes in coffee fermentation and their impact on coffee quality, J. Food Qual. 2019 (2019) 1–6, http://dx.doi.org/10.1155/2019/4836709.

[5] N. Cordoba, M. Fernandez-Alduenda, F.L. Moreno, Y. Ruiz, Coffee extraction: A review of parameters and their influence on the physicochemical characteristics and flavour of coffee brews, Trends Food Sci. Technol. 96 (2020) 45–60, http://dx.doi.org/10.1016/j.tifs.2019.12.004.

[6] A.E. Peñuela-Martínez, S. Moreno-Riascos, R. Medina-Rivera, Influence of temperature-controlled fermentation on the quality of mild coffee (coffea arabica L.) cultivated at different elevations, Agriculture 13 (2023) 1132, http://dx.doi.org/10.3390/agriculture13061132.

[7] A.F.S. Pino, Z.Y.D. Espinosa, E.V.R. Cabrera, Characterization of the rhizosphere bacterial microbiome and coffee bean fermentation in the castillo-tambo and bourbon varieties in the popayán-Colombia plateau, BMC Plant Biol. 23 (2023) 217, http://dx.doi.org/10.1186/s12870-023-04182-2.

[8] I. Prakash, S.S. R., S.H. P., P. Kumar, H. Om, K. Basavaraj, P.S. Murthy, Metabolomics and volatile fingerprint of yeast fermented robusta coffee: A value added coffee, LWT 154 (2022) 112717, http://dx.doi.org/10.1016/j.lwt.2021.112717.

[9] K. Aswathi, A. Shirke, A. Praveen, S.R. Chaudhari, P.S. Murthy, Pulped natural/honey robusta coffee fermentation metabolites, physico-chemical and sensory profiles, Food Chem. 429 (2023) 136897, http://dx.doi.org/10.1016/j.foodchem.2023.136897.

[10] R. Mahingsapun, P. Tantayotai, T. Panyachanakul, S. Samosorn, K. Dolsophon, R. Jiamjariyatam, W. Lorliam, N. Srisuk, S. Krajangsang, Enhancement of arabica coffee quality with selected potential microbial starter culture under controlled fermentation in wet process, Food Biosci. 48 (2022) 101819, http://dx.doi.org/10.1016/j.fbio.2022.101819.

[11] G. Iatropoulos, P. Herman, A. Lansner, J. Karlgren, M. Larsson, J.K. Olofsson, The language of smell: Connecting linguistic and psychophysical properties of odor descriptors, Cognition 178 (2018) 37–49, http://dx.doi.org/10.1016/j.cognition.2018.05.007.

[12] K. Toko, Taste sensor with global selectivity, Mater. Sci. Eng. C 4 (1996) 69–82, http://dx.doi.org/10.1016/0928-4931(96)00134-8.

[13] S. Takagi, K. Toko, K. Wada, H. Yamada, K. Toyoshima, Detection of suppression of bitterness by sweet substance using a multichannel taste sensor, J. Pharm. Sci. 87 (1998) 552–555, http://dx.doi.org/10.1021/js970429x.

[14] M.M. Ali, N. Hashim, S.A. Aziz, O. Lasekan, Principles and recent advances in electronic nose for quality inspection of agricultural and food products, Trends Food Sci. Technol. 99 (2020) 1–10, http://dx.doi.org/10.1016/j.tifs.2020.02.028.

[15] X. Yang, Y. Liu, L. Mu, W. Wang, Q. Zhan, M. Luo, H. Tian, C. Lv, J. Li, Discriminant research for identifying aromas of non-fermented pu-erh tea from different storage years using an electronic nose, J. Food Process. Preservat. 42 (2018) e13721, http://dx.doi.org/10.1111/jfpp.13721.

[16] J. Chen, J. Gu, R. Zhang, Y. Mao, S. Tian, Freshness evaluation of three kinds of meats based on the electronic nose, Sensors 19 (2019) 605, http://dx.doi.org/10.3390/s19030605.

[17] J. Tan, W.L. Kerr, Characterizing cocoa refining by electronic nose using a kernel distribution model, LWT 104 (2019) 1–7, http://dx.doi.org/10.1016/j.lwt.2019.01.028.

[18] W. Dong, R. Hu, Y. Long, H. Li, Y. Zhang, K. Zhu, Z. Chu, Comparative evaluation of the volatile profiles and taste properties of roasted coffee beans as affected by drying method and detected by electronic nose, electronic tongue, and HS-SPME-GC-MS, Food Chem. 272 (2019) 723–731, http://dx.doi.org/10.1016/j.foodchem.2018.08.068.

[19] R.L.F. Filho, F.O. Barino, J. Calderano, Í.F.V. Alvarenga, D. Campos, A.B. dos Santos, In-fiber mach–zehnder interferometer as a promising tool for optical nose and odor prediction during the fermentation process, Opt. Lett. 48 (2023) 3905, http://dx.doi.org/10.1364/OL.486742.

[20] S. Boesveldt, M.J. Olsson, J.N. Lundström, Carbon chain length and the stimulus problem in olfaction, Behav. Brain Res. 215 (2010) 110–113, http://dx.doi.org/10.1016/j.bbr.2010.07.007.

[21] A. Keller, R.C. Gerkin, Y. Guan, A. Dhurandhar, G. Turu, B. Szalai, J.D. Mainland, Y. Ihara, C.W. Yu, R. Wolfinger, C. Vens, leander schietgat, K.D. Grave, R. Norel, G. Stolovitzky, G.A. Cecchi, L.B. Vosshall, pablo meyer, Predicting human olfactory perception from chemical features of odor molecules, Science 355 (2017) 820–826, http://dx.doi.org/10.1126/science.aal2014.

[22] T. Debnath, T. Nakamoto, Predicting human odor perception represented by continuous values from mass spectra of essential oils resembling chemical mixtures, PLoS One 15 (2020) e0234688, http://dx.doi.org/10.1371/journal.pone.0234688.

[23] A.D. Wilson, Review of electronic-nose technologies and algorithms to detect hazardous chemicals in the environment, Proc. Technol. 1 (2012) 453–463, http://dx.doi.org/10.1016/j.protcy.2012.02.101.
[24] R.L.F. Filho, A.B. dos Santos, A.P.L. Barbero, V.N.H. Silva, Optical inclinometer based on a LPG-taper series configuration, J. Microw. Optoelectron. Electromagn. Appl. 20 (2021) 612–620, http://dx.doi.org/10.1590/2179-10742021v20i3254754.
[25] B. Li, L. Jiang, S. Wang, H.-L. Tsai, H. Xiao, Femtosecond laser fabrication of long period fiber gratings and applications in refractive index sensing, Opt. Laser Technol. 43 (2011) 1420–1423, http://dx.doi.org/10.1016/j.optlastec.2011.04.011.
[26] L. Qi, C.-L. Zhao, J. Yuan, M. Ye, J. Wang, Z. Zhang, S. Jin, Highly reflective long period fiber grating sensor and its application in refractive index sensing, Sensors Actuators B 193 (2014) 185–189, http://dx.doi.org/10.1016/j.snb.2013.11.063.
[27] J. Yan, J. Feng, J. Ge, J. Chen, F. Wang, C. Xiang, D. Wang, Q. Yu, H. Zeng, Highly sensitive humidity sensor based on a GO/Co-MOF-74 coated long period fiber grating, IEEE Photonics Technol. Lett. 34 (2022) 77–80, http://dx.doi.org/10.1109/LPT.2021.3139114.
[28] Y. Wang, Y. Liu, F. Zou, C. Jiang, C. Mou, T. Wang, Humidity sensor based on a long-period fiber grating coated with polymer composite film, Sensors 19 (2019) 2263, http://dx.doi.org/10.3390/s19102263.
[29] B. Xu, J. Huang, X. Xu, A. Zhou, L. Ding, Ultrasensitive NO gas sensor based on the graphene oxide-coated long-period fiber grating, ACS Appl. Mater. Interfaces 11 (2019) 40868–40874, http://dx.doi.org/10.1021/acsami.9b14212.
[30] X. Qin, W. Feng, X. Yang, J. Wei, G. Huang, Molybdenum sulfide/citric acid composite membrane-coated long period fiber grating sensor for measuring trace hydrogen sulfide gas, Sensors Actuators B 272 (2018) 60–68, http://dx.doi.org/10.1016/j.snb.2018.05.152.
[31] R. Falate, K. Nike, P.R. da Costa Neto, E. Cação Jr., M. Muller, H.J. Kalinowski, J.L. Fabris, Alternative technique for biodiesel quality control using an optical fiber long-period grating sensor, Quí Mica Nova 30 (2007) 1677–1680, http://dx.doi.org/10.1590/S0100-40422007000700034.
[32] Y.-G. Han, B.H. Lee, W.-T. Han, U.-C. Paek, Y. Chung, Fibre-optic sensing applications of a pair of long-period fibre gratings, Meas. Sci. Technol. 12 (2001) 778–781, http://dx.doi.org/10.1088/0957-0233/12/7/304.
[33] P. Li, M. Wang, J. Fu, J. Shi, Z. Zhu, J. Yang, C. Guan, L. Yuan, Bend-compensated long period grating in hole-assisted eccentric-core fiber, Opt. Commun. 434 (2019) 19–22, http://dx.doi.org/10.1016/j.optcom.2018.10.012.
[34] F. Esposito, A. Srivastava, A. Iadicicco, S. Campopiano, Multi-parameter sensor based on single long period grating in panda fiber for the simultaneous measurement of SRI, temperature and strain, Opt. Laser Technol. 113 (2019) 198–203, http://dx.doi.org/10.1016/j.optlastec.2018.12.022.
[35] T. Erdogan, Fiber grating spectra, J. Lightwave Technol. 15 (1997) 1277–1294, http://dx.doi.org/10.1109/50.618322.
[36] X. Shu, L. Zhang, I. Bennion, Sensitivity characteristics of long-period fiber gratings, J. Lightwave Technol. 20 (2002) 255–266, http://dx.doi.org/10.1109/50.983240.
[37] O. Frazão, R. Falate, J.L. Fabris, J.L. Santos, L.A. Ferreira, F.M. Araújo, Optical inclinometer based on a single long-period fiber grating combined with a fused taper, Opt. Lett. 31 (2006) 2960, http://dx.doi.org/10.1364/OL.31.002960.
[38] X. Liu, J. Long, Y. Ding, Y. Hu, Z. Du, B. Xu, D. Deng, Measuring the refractive index of scintillation crystal with a mach-zehnder interferometer, Opt. Contin. 1 (2022) 909, http://dx.doi.org/10.1364/OPTCON.453688.
[39] F. Esposito, A. Srivastava, S. Campopiano, A. Iadicicco, Sensing features of arc-induced long period gratings, in: 7th International Symposium on Sensor Science, MDPI, Basel Switzerland, 2019, p. 29, http://dx.doi.org/10.3390/proceedings2019015029.
[40] A. Martinez-Rios, D. Monzon-Hernandez, I. Torres-Gomez, Highly sensitive cladding-etched arc-induced long-period fiber gratings for refractive index sensing, Opt. Commun. 283 (2010) 958–962, http://dx.doi.org/10.1016/j.optcom.2009.10.108.
[41] B. Li, L. Jiang, S. Wang, Q.C.M. Wang, J. Yang, A new mach-zehnder interferometer in a thinned-cladding fiber fabricated by electric arc for high sensitivity refractive index sensing, Opt. Lasers Eng. 50 (2012) 829–832, http://dx.doi.org/10.1016/j.optlaseng.2012.01.024.
[42] T. Zhu, D. Wu, M. Deng, D. Duan, Y. Rao, X. Bao, Refractive index sensing based on mach-zehnder interferometer formed by three cascaded single-mode fiber tapers, 2011, p. 77532P, http://dx.doi.org/10.1117/12.884842.
[43] H.M. Bae, M. Haile, W.H. Kang, Evaluation of antioxidant, organic acid, and volatile compounds in coffee pulp wine fermented with native yeasts isolated from coffee cherries, Food Sci. Technol. Int. 28 (2022) 716–727, http://dx.doi.org/10.1177/10820132211051874.
[44] R.C. O'Byrne, N.P. Gambasica, S.A. Forero, Physicochemical, microbiological, and sensory analysis of fermented coffee from sierra nevada of santa marta, Colombia, Coffee Scienc. 15 (2020) 1–6, http://dx.doi.org/10.25186/.v15i.1797.
[45] M.C.B. da Mota, N.N. Batista, D.R. Dias, R.F. Schwan, Impact of microbial self-induced anaerobiosis fermentation (SIAF) on coffee quality, Food Biosci. 47 (2022) 101640, http://dx.doi.org/10.1016/j.fbio.2022.101640.
[46] S.S. R., S.H. P., I. Prakash, M. Khan, H.N. Punil Kumar, H. Om, K. Basavaraj, P.S. Murthy, Microbial ecology and functional coffee fermentation dynamics with pichia kudriavzevii, Food Microbiol. 105 (2022) 104012, http://dx.doi.org/10.1016/j.fm.2022.104012.
[47] G. Rego, Arc-induced long period fiber gratings, J. Sens. 2016 (2016) 1–14, http://dx.doi.org/10.1155/2016/3598634.
[48] G. Rego, O. Okhotnikov, E. Dianov, V. Sulimov, High-temperature stability of long-period fiber gratings produced using an electric arc, J. Lightwave Technol. 19 (2001) 1574–1579, http://dx.doi.org/10.1109/50.956145.
[49] R. Luiz, D. Campos, F.d. Delgado, A.B. dos Santos, Long-period fiber grating embedded in polymer structure for deformation monitoring, Appl. Phys. B 127 (2021) 163, http://dx.doi.org/10.1007/s00340-021-07712-8.
[50] F.O. Barino, R.L. Faraco-Filho, D. Campos, A.B. dos Santos, 3D-printed force sensitive structure using embedded long-period fiber grating, Opt. Laser Technol. 148 (2022) 107697, http://dx.doi.org/10.1016/j.optlastec.2021.107697.
[51] J. Meng, Y. Yang, Symmetrical two-dimensional PCA with image measures in face recognition, Int. J. Adv. Robot. Syst. 9 (2012) 238, http://dx.doi.org/10.5772/54014.
[52] S. Karamizadeh, S.M. Abdullah, A.A. Manaf, M. Zamani, A. Hooman, An overview of principal component analysis, J. Signal Inf. Process. 04 (2013) 173–175, http://dx.doi.org/10.4236/jsip.2013.43B031.

Renato Luiz Faraco Filho was born in Conselheiro Lafaiete, Brazil, in 1997. He received the B.Sc. degree in electronics from the Federal University of Juiz de Fora (UFJF), Minas Gerais, Brazil, in 2022, where he is currently pursuing the M.Sc. degree in electrical engineering with the Programa de Pós-Graduação em Engenharia Elétrica (PPEE). His current research interests include instrumentation, optical fiber sensors, and machine learning.

João Victor de Castro was born in Santos Dumont, Brazil, in 2003. He is currently pursuing the B.Sc. degree in electrical engineering and robotics and industrial automation with the Federal University of Juiz de Fora. His current research interests include instrumentation, optical fiber sensors, and computational methods.

Felipe Oliveira Barino was born in Juiz de Fora, Brazil, in 1996. He received the B.S. and M.Sc. degrees in electronics from the Federal University of Juiz de Fora (UFJF), Juiz de Fora, in 2019 and 2021, respectively. He is currently pursuing the Ph.D. degree in electrical engineering at the same institution, with the Pós-Graduação em Engenharia Elétrica (PPEE). His current research interests are related to instrumentation, metrology, machine learning, transfer learning, optical fiber sensors, and sensor packaging.

Deivid E. Campos was born in São João Nepomuceno, Brazil, in the year 1991. His academic journey is noteworthy, having earned a Bachelor's degree in Exact Sciences in 2014, and subsequently, in 2022, a Bachelor's degree in Mechanical Engineering, both awarded by the Federal University of Juiz de Fora (UFJF), situated in the state of Minas Gerais, Brazil. Currently, he is immersed in a Master's program in Computational Modeling at the same institution. His research interests encompass areas of significant relevance in the current scientific landscape, involving advanced instrumentation, high-tech fiber optic sensors, the intricacies of three-dimensional modeling with 3D printing, and Machine Learning.

Alexandre Bessa dos Santos was born in Juiz de Fora, Brazil, in 1975. He received the M.Sc. and Ph.D. degrees in electrical engineering from Pontifical Catholic University (PUC), Rio de Janeiro, Brazil, in 2001 and 2005, respectively. Since 2010, he has been an Associate Professor with the Department of Circuits, Federal University of Juiz de Fora (UFJF), Juiz de Fora. His research interests include applied electromagnetism, optical sensors, computational methods, instrumentation, and metrology